Mutations in GREB1L Cause Bilateral Kidney Agenesis in Humans and Mice

Lara de Tomasi, Pierre David, Camille Humbert, Flora Silbermann, Christelle Arrondel, Frédéric Tores, Stéphane Fouquet, Audrey Desgrange, Olivier Niel, Christine Bole-Feysot, et al.

Mutations in *GREB1L* Cause Bilateral Kidney Agenesis in Humans and Mice

Lara De Tomasi,[1,2,3] Pierre David,[4] Camille Humbert,[1,2] Flora Silbermann,[1,2] Christelle Arrondel,[1,2] Frédéric Tores,[5] Stéphane Fouquet,[6] Audrey Desgrange,[2,7] Olivier Niel,[8] Christine Bole-Feysot,[9] Patrick Nitschké,[5] Joëlle Roume,[10] Marie-Pierre Cordier,[11] Christine Pietrement,[12] Bertrand Isidor,[13] Philippe Khau Van Kien,[14] Marie Gonzales,[15] Marie-Hélène Saint-Frison,[16] Jelena Martinovic,[17] Robert Novo,[18] Juliette Piard,[19] Christelle Cabrol,[19] Ishwar C. Verma,[20] Ratna Puri,[20] Hubert Journel,[21] Jacqueline Aziza,[22] Laurent Gavard,[23] Marie-Hélène Said-Menthon,[24] Laurence Heidet,[25,26] Sophie Saunier,[1,2] and Cécile Jeanpierre[1,2,*]

Congenital anomalies of the kidney and urinary tract (CAKUT) constitute a major cause of chronic kidney disease in children and 20% of prenatally detected anomalies. CAKUT encompass a spectrum of developmental kidney defects, including renal agenesis, hypoplasia, and cystic and non-cystic dysplasia. More than 50 genes have been reported as mutated in CAKUT-affected case subjects. However, the pathophysiological mechanisms leading to bilateral kidney agenesis (BKA) remain largely elusive. Whole-exome or targeted exome sequencing of 183 unrelated familial and/or severe CAKUT-affected case subjects, including 54 fetuses with BKA, led to the identification of 16 heterozygous variants in *GREB1L* (growth regulation by estrogen in breast cancer 1-like), a gene reported as a target of retinoic acid signaling. Four loss-of-function and 12 damaging missense variants, 14 being absent from GnomAD, were identified. Twelve of them were present in familial or simplex BKA-affected case subjects. Female BKA-affected fetuses also displayed uterus agenesis. We demonstrated a significant association between *GREB1L* variants and BKA. By *in situ* hybridization, we showed expression of *Greb1l* in the nephrogenic zone in developing mouse kidney. We generated a *Greb1l* knock-out mouse model by CRISPR-Cas9. Analysis at E13.5 revealed lack of kidneys and genital tract anomalies in male and female $Greb1l^{-/-}$ embryos and a slight decrease in ureteric bud branching in $Greb1l^{+/-}$ embryos. We showed that *Greb1l* invalidation in mIMCD3 cells affected tubulomorphogenesis in 3D-collagen culture, a phenotype rescued by expression of the wild-type human protein. This demonstrates that *GREB1L* plays a major role in early metanephros and genital development in mice and humans.

Congenital anomalies of the kidney and urinary tract (CAKUT) comprise a broad spectrum of renal and urinary tract malformations of various severity. CAKUT defects range from complete renal agenesis to renal hypodysplasia, multicystic kidney dysplasia, duplex renal collecting system, ureteropelvic junction obstruction, megaureter, and posterior urethral valve. Altogether, CAKUT occur in about 1 in 500 live births and account for 15%–20% of congenital anomalies detected *in utero*.[1] They represent a major cause of chronic kidney disease in children,[2] and the most severe cases are associated with perinatal lethality and may lead to termination of pregnancy. CAKUT are due to defects arising during kidney development.[3] Differentiation of the metanephros (definitive kidney) is initiated by a reciprocal induction between the ureteric bud (UB) protruding from the Wolffian duct and the metanephric mesenchyme (MM), that control branching of the UB for formation of the collecting ducts and mesenchymal-to-epithelial transition of the MM for differentiation of the nephrons.[4] The pathophysiological mechanisms leading to CAKUT by affecting nephrogenesis processes are complex, involving both environmental and genetic

[1]Laboratory of Hereditary Kidney Diseases, INSERM UMR 1163, Imagine Institute, 75015 Paris, France; [2]Paris Descartes-Sorbonne Paris Cité University, Imagine Institute, 75015 Paris, France; [3]Paris Diderot University, 75013 Paris, France; [4]Transgenesis Platform, Laboratoire d'Expérimentation Animale et Transgenèse (LEAT), Imagine Institute, Structure Fédérative de Recherche Necker INSERM US24/CNRS UMS3633, 75015 Paris, France; [5]Bioinformatic Platform, INSERM UMR 1163, Paris Descartes-Sorbonne Paris Cité University, Imagine Institute, 75015 Paris, France; [6]Imaging Platform, Sorbonne Universités, UPMC Univ Paris 06, INSERM UMR_S968 and CNRS UMR7210, Institut de la Vision, 75012 Paris, France; [7]Laboratory of Heart Morphogenesis, INSERM UMR 1163, Imagine Institute-Pasteur Institute, 75015 Paris, France; [8]APHP, Pediatric Nephrology Department, Hôpital Robert Debré, 75019 Paris, France; [9]Genomic Platform, INSERM UMR 1163, Paris Descartes-Sorbonne Paris Cité University, Imagine Institute, 75015 Paris, France; [10]Unité de Génétique Médicale, Centre de Référence des Maladies rares du Développement (AnD DI Rares), CHI Poissy - St Germain en Laye, 78300 Poissy, France; [11]Service de Génétique, Groupement Hospitalier Est, 69677 Bron, France; [12]Unité de Néphrologie Pédiatrique, CHU Reims, 51100 Reims, France; [13]Service de Génétique Médicale, CHU Nantes, 44093 Nantes, France; [14]Unité de Génétique Médicale, Nîmes University Hospital, CHU Carémeau, 30900 Nîmes, France; [15]APHP, Département de Génétique Médicale, Hôpital Armand Trousseau, Université Pierre et Marie Curie, 75571 Paris, France and APHP, Unité d'EmbryoFœtopathologie, Service d'Histologie-Embryologie-Cytogénétique, Hôpital Necker-Enfants Malades, 75015 Paris, France; [16]APHP, Département de Génétique, Unité de Fœtopathologie, Hôpital Robert Debré, 75019 Paris, France; [17]APHP, Unit of Fetal Pathology, Antoine Béclère Hospital, 92140 Clamart, France; [18]Centre Hospitalier Universitaire de Lille, Hôpital Jeanne de Flandre, Service de Néphrologie Pédiatrique, 59000 Lille, France; [19]Centre de Génétique Humaine, CHU Besançon, Université de Franche-Comté, 25000 Besançon, France; [20]Institute of Medical Genetics and Genomics, Sir Ganga Ram Hospital, New Delhi 110060, India; [21]Service de Génétique Médicale, Hôpital Chubert, 56000 Vannes, France; [22]Département d'Anatomie et Cytologie Pathologiques, IUCT-Oncopole, 31100 Toulouse, France; [23]Service de Gynécologie-Obstétrique, Hôpital Louis Mourier, 92700 Colombes, France; [24]Service de Pédiatrie, Hôpitaux du Léman, 74203 Thonon les Bains, France; [25]APHP, Centre de Référence des Maladies Rénales Héréditaires de l'Enfant et de l'Adulte (MARHEA), Hôpital Necker-Enfants Malades, 75015 Paris, France; [26]APHP, Service de Néphrologie Pédiatrique, Hôpital Necker-Enfants Malades, 75015 Paris, France

*Correspondence: cecile.jeanpierre@inserm.fr

https://doi.org/10.1016/j.ajhg.2017.09.026.

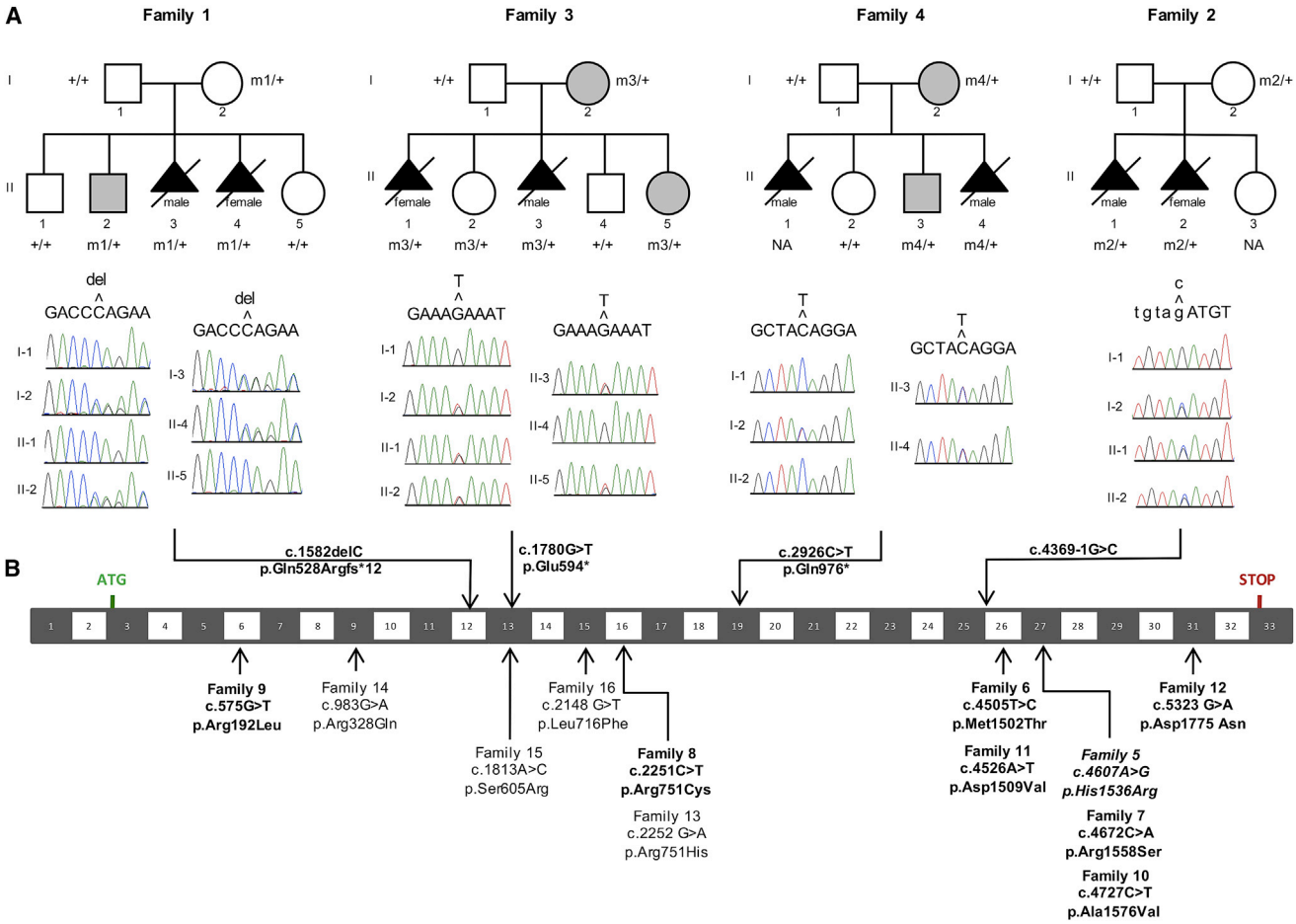

Figure 1. Identification of *GREB1L* Heterozygous Loss-of-Function and Missense Variants in 16 CAKUT-Affected Families, 12 of Them with Fetuses with Bilateral Kidney Agenesis

(A) Pedigrees of the four families with loss-of-function mutations. Case subjects presenting with bilateral and unilateral kidney agenesis are in black and gray, respectively. Families 1 and 2 were analyzed by whole-exome sequencing and families 3 and 4 by targeted exome sequencing. Validation of the mutations and segregation analysis were performed by Sanger sequencing. Position of the mutations are indicated by arrows on the chromatograms. NA, individual with non available DNA.

(B) Representation of *GREB1L* cDNA with the exonic positions of the 4 loss-of-function (above) and the 12 missense (below) variants. Mutations identified in BKA-affected case subjects are indicated in bold and the mutation that appeared *de novo* in a mother in italics. Pedigrees of these 12 families with missense variants are shown in Figure S1.

factors. The existence of a genetic component for CAKUT was proposed based on the observation of familial and syndromic cases. A large range of genetic heterogeneity has been highlighted by the identification of mutations, mostly at the heterozygous state, in more than 50 genes, many of them encoding transcription factors with a crucial role during nephrogenesis (e.g., *HNF1B* [MIM: 189907], *PAX2* [MIM: 167409], *EYA1* [MIM: 601653], *SIX1* [MIM: 601205], *SALL1* [MIM: 602218], *GATA3* [MIM: 131320], and *PBX1* [MIM: 176310]).[5–7] Among these ~50 genes, few are associated with bilateral kidney agenesis (BKA) in human. Mutations have been reported in *ANOS1* (MIM: 300836), *EYA1*, *FGF20* (MIM: 615721), *ITGA8* (MIM: 191830), and *RET* (MIM: 164761) in some case subjects with isolated BKA, or in *KIF14* (MIM: 616258), *FRAS1* (MIM: 219000), and *FREM1* (MIM: 608980) in syndromic forms.[5,8–12] However, in most BKA-affected fetuses, even when a monogenic cause is likely according to the genealogy, the mutated gene is unknown.

In order to identify additional genes mutated in CAKUT, 30 case subjects from 15 families were analyzed by whole-exome sequencing (WES). Among these 15 families, 11 included fetuses with BKA. Written informed consent was obtained from all individuals and/or from parents and approved by the "Comité de Protection des Personnes pour la Recherche Biomédicale Ile de France II." In two of these families, we identified heterozygous loss-of-function mutations in *GREB1L* (growth regulation by estrogen in breast cancer 1-like; GenBank: NM_001142966.2), a gene reported as a target of retinoic acid signaling[13] (Figure 1, Table 1). In family 1, analyzed by combined WES and linkage analysis (Table S1), we identified a single base pair deletion (c.1582delC) leading to a frameshift (p.Gln528Argfs*12) in the two fetuses affected with BKA (II-3 and II-4 in Figure 1A) and their alive brother (II-2)

Table 1. Identification of Heterozygous Variants in *GREB1L* (GenBank: NM_001142966.2) in 16 CAKUT-Affected Case Subjects and Families

Fam	NGS	Case Subjects with Kidney Phenotype	Other Defects	Mutation (Chrom Position)[a]	Mutation (Nucleotide)	Substitution (Amino Acid)	GnomAD	Nucleotide Conservation (phred)	Amino Acid Conservation	PP2	Sift	Grantham	CADD (phred)	Inheritance
1	WES	2 fetuses: BKA (M/F) 1 child: UKA (M)	male fetus: clinodactyly (5th fingers) female fetus: clinodactyly (5th fingers), absence of uterus; mother: unicornuated uterus	18:19029659	c.1582delC	p.Gln528Argfs*12	absent	–	–	–	–	–	34	maternal[b]
2	WES	2 fetuses: BKA (M/F)	male fetus: thickened left ventricular wall, 10 pairs of ribs female fetus: absence of uterus	18:19088078	c.4369−1G>C	–	absent	–	–	–	–	–	25.2	maternal[b]
3	TES	2 fetuses: BKA (M/F) 1 child: UKA+VUR (F) mother: UKA	female fetus: absence of uterus and fallopian trumps affected child: ovarian hernia mother: absence of uterine left artery	18:19031043	c.1780G>T	p.Glu594*	absent	–	–	–	–	–	40	maternal
4	TES	2 fetuses: BKA (M/M) 1 child: UKA (M) mother: UKA	none	18:19070208	c.2926C>T	p.Gln976*	absent	–	–	–	–	–	40	maternal
5	TES	2 fetuses: BKA (F), UKA+MCD (M) mother: horseshoe kidney	female fetus: 11 pairs of ribs, absence of uterus	18:19088424	c.4607A>G	p.His1536Arg	absent	4.81	zebrafish	0.955	0.07	29	23.3	maternal
6	TES	fetus: BKA (M)	retro-esophageal subclavian artery, adrenal gland hypoplasia, enlarged thymus, one pair of cervical ribs	18:19088215	c.4505T>C	p.Met1502Thr	absent	3.11	zebrafish	0.892	0	81	24.8	maternal[c]
7	TES	fetus: BKA (F)	none	18:19088489	c.4672C>A	p.Arg1558Ser	absent	3.51	zebrafish	0.908	0.01	110	34	maternal[b]
8	TES	2 fetuses: BKA mother: unilateral hypoplasia	mother: unicornuated uterus	18:19053060	c.2251C>T	p.Arg751Cys	absent	3.51	zebrafish	0.998	0	180	34	maternal
9	TES	fetus: BKA (M) mother: UKA	mother: ID diabetes, unique fallopian trump and ovary	18:18981153	c.575G>T	p.Arg192Leu	absent	6.26	zebrafish	0.999	0.34	102	26.1	maternal
10	TES	fetus: BKA (M)	auricular tag, hypertrophic left ventricle, aortic stenosis	18:19088544	c.4727C>T	p.Ala1576Val	absent	5.86	tetraodon	0.947	0	64	33	UNK

(*Continued on next page*)

Table 1. *Continued*

Fam	NGS	Case Subjects with Kidney Phenotype	Other Defects	Mutation (Chrom Position)[a]	Mutation (Nucleotide)	Substitution (Amino Acid)	GnomAD	Nucleotide Conservation (phred)	Amino Acid Conservation	PP2	Sift	Grantham	CADD (phred)	Inheritance
11	TES	fetus: BKA (M)	adrenal cytomegaly	18:19088236	c.4526A>T	p.Asp1509Val	6.584×10^{-6}	2.06	zebrafish	0.835	0	152	26.3	UNK
12	TES	fetus: BKA (M)	preauricular tag, lop ear	18:19098046	c.5323 G>A	p.Asp1775Asn	absent	5.69	zebrafish	0.999	0	23	34	UNK
13	TES	fetus: UKA+MCD, megaurethra (M)	hepatic portal fibrosis	18:19053061	c.2252 G>A	p.Arg751His	2.697×10^{-5}	6.34	zebrafish	0.996	0	29	34	maternal[c]
14	TES	fetus: pelvic kidney+MCD (M) mother: VUR	none	18:19020263	c.983G>A	p.Arg328Gln	absent	4.64	zebrafish	0.999	0.01	43	34	maternal
15	TES	adult: UKA+ multilocular cyst (F)	blind ending hemi-vagina and bicornuated uterus	18:19031076	c.1813A>C	p.Ser605Arg	absent	4.81	zebrafish	0.992	0.07	110	24.8	paternal[b]
16	TES	child: VUR (M)	iris anomaly	18:19034490	c.2148 G>T	p.Leu716Phe	absent	3.84	zebrafish	0.525	0.04	22	24.5	UNK

Abbreviations are as follows: Fam, family; NGS, next generation sequencing; WES, whole-exome sequencing; TES, targeted exome sequencing; BKA, bilateral kidney agenesis; UKA, unilateral kidney agenesis; MCD, multicystic dysplasia; VUR, vesicoureteral reflux; M, male; F, female; ID, insulin-dependent; UNK, unknown; PP2, PolyPhen2; CADD, Combined Annotation Dependent Depletion.
[a]Position on GRCh37/hg19 human genome assembly.
[b]Parent with normal renal ultrasound.
[c]Mother with renal status non ascertained by renal ultrasound.

with unilateral kidney agenesis (UKA). In family 2, WES performed in the two fetuses with BKA (II-1 and II-2) identified a 3′ splice mutation (c.4369−1G>C). Although no RNA was available to test the effect of this variant, it was predicted to lead to skipping of exon 26 and result in an in-frame deletion of 54 amino acids. These two variations were absent from GnomAD and our in-house database. In order to look for additional mutations in *GREB1L*, probes covering the 33 exons of the gene were designed and added to a previously described SureSelect panel of 330 genes used for molecular diagnosis of CAKUT-affected case subjects.[5] Analysis of 168 unrelated case subjects with no causative mutation identified, 43 of which presented with BKA, led to the identification of 14 heterozygous variations in *GREB1L*, including 2 nonsense mutations and 12 missense variants affecting conserved amino acids and predicted as damaging (CADD scores > 20) (Figures 1 and S1, Table 1). Twelve of these variants were absent from GnomAD and our in-house database, while two missense variants were present in GnomAD with very low frequencies (6.5×10^{-6} and 2.7×10^{-7}). The two nonsense mutations, c.1780G>T (p.Glu594*) and c.2926C>T (p.Gln976*), identified in families 3 and 4, respectively, were present in all BKA-affected fetuses with available DNA (II-1 and II-3 in family 3, II-4 in family 4) and in family members with UKA (II-5 in family 3, II-3 in family 4) (Figure 1, Table 1). Eight of the 12 missense variants were also identified in BKA-affected fetuses in families 5 to 12 (II-6 in family 5, II-3 in family 6, II-1 in families 7, 10, 11, and 12, II-2 in families 8 and 9) (Figure S1, Table 1). Five of these missense variants were located in exon 26 (the exon predicted to be skipped in family 2) or exon 27, suggesting that this region was crucial for the function of the protein (Figure 1B). In 11 of the 12 families with available parental DNA, the variation was inherited from the mother, either presenting with CAKUT phenotype (families 3, 4, 5, 8, 9, and 14) or with normal renal ultrasound (families 1, 2, and 7) (Figures 1A and S1). In families 6 and 13 the status of the mother had not been ascertained by renal ultrasound. In family 5, analysis of DNA from the maternal grandparents showed that the mutation carried by the mother with horseshoe kidney occurred *de novo* (Figure S1). Two hypotheses can be proposed to explain the observed maternal bias in transmission of *GREB1L* mutations. The first one is genomic imprinting of *GREB1L*, with specific expression of the maternal allele during kidney development (paternally imprinted gene). Imprinting of genes with a role during kidney development has already been reported.[14,15] In this hypothesis, only mutations inherited from the mother would result in a phenotype. The second hypothesis is that *GREB1L* mutations would affect male fertility, explaining the very low rate of paternal inheritance. In favor of this hypothesis, the only paternally inherited variant, in family 15, was associated with a mild phenotype (unilateral agenesis and multilocular cyst in adult individual II-1; Figure S1), suggesting that it would

be a hypomorphic mutation that would not affect male fertility.

Absence of kidney defect, ascertained by renal ultrasound, in four parents harboring a variant (families 1, 2, 7, and 15) and two children harboring a variant (individuals II-2 in families 3 and 14) suggests incomplete penetrance. As for family 9, the *GREB1L* variant identified in the male fetus with BKA (II-2, Figure S1) and in his mother, presenting with UKA and unilateral ovary and fallopian trump agenesis, was absent from his sister fetus (II-1) also affected with BKA. Although we cannot exclude that the *GREB1L* variant identified in this family might not be pathogenic, different mechanisms could have led to BKA in the two fetuses. Indeed, the mother presented with poorly controlled insulin-dependent diabetes, a condition known to increase the risk of renal developmental defects.[16]

Altogether, 12 of the 16 families with *GREB1L* variants comprised BKA-affected fetuses, notably the 4 with loss-of-function mutations. CAKUT phenotype in the four other families was severe fetal defects in two case subjects (UKA or ectopic kidney plus multicystic dysplasia) or milder phenotype in the two last case subjects (UKA + multilocular cyst, or vesicoureteral reflux) (Table 1). As frequently observed for CAKUT and other developmental defects transmitted as autosomal-dominant traits, *GREB1L* loss-of-function and missense mutations were associated with intrafamilial variable expressivity, from lethal to mild CAKUT phenotype. We observed genital tract defects with variable severity in females, ranging from uterus agenesis (four of the five female BKA fetuses) to milder defects in mothers harboring variants (unicornuated uterus in two mothers unilateral ovarian and fallopian trump agenesis in one mother), suggesting that *GREB1L* mutations also affect female genital development. No overt genital defect was identified in the male fetuses. Finally, other non-renal defects were present in several fetuses, notably abnormal number of ribs (three fetuses), heart defect (two fetuses), enlarged thymus (one fetus), and hepatic fibrosis (one fetus) (Table 1). Similar to many other genes in which mutations lead to CAKUT,[17] mutations in *GREB1L* could thus lead to both isolated and syndromic disease.

In order to evaluate the enrichment in *GREB1L*, rare (absent from GnomAD) damaging variants in CAKUT-affected case subjects, we compared the number of loss-of-function/damaging missense variants in case versus control subjects. For the affected individuals we considered 183 case subjects (one affected case subject for each of the 15 families analyzed by WES plus the 168 unrelated case subjects analyzed by targeted sequencing, including a total of 54 BKA-affected fetuses). For the control subjects, we used 361 unrelated individuals who were unaffected parents of children presenting with immune deficiency sequenced by WES on the same genomic platform. We ensured that all 31 coding *GREB1L* exons were fully covered to allow variant identification. In most of the samples (177 case subjects and 337 control subjects), mean coverage was >20× for all the exons, while in 30 samples (6 case subjects, 24 control subjects), one or two exons had mean coverage <20×, with a minimum base coverage ≥10. Variants were selected using Variant Tools and Variant Association Tools.[18,19] Using combined and multivariate collapsing (CMC) test,[20] we demonstrated a significant association between rare *GREB1L* variants and CAKUT phenotype (loss-of-function plus missense: $p = 1.9 \times 10^{-4}$; missense: $p = 5.0 \times 10^{-3}$) (Table S2). No *GREB1L* loss-of-function variants were identified in the 361 individuals of the control cohort or in >5,000 non-CAKUT case subjects of our entire in-house database, and such variants were very rare in the GnomAD database, supporting their deleterious effect. Finally, we sought to analyze the association between *GREB1L* mutations and BKA in our CAKUT cohort (Table S2). Indeed, among the 54 BKA-affected case subjects, 12 (25.8%) were carrying a variant in *GREB1L*. Statistical analysis demonstrated a highly significant association, whenever considering loss-of-function plus missense variants ($p = 6.1 \times 10^{-5}$) or only missense variants ($p = 4.5 \times 10^{-3}$).

GREB1L encodes a poorly characterized protein, named because of its high level of similarity with *GREB1* (growth regulation by estrogen in breast cancer 1).[21] Another gene encoding a nuclear receptor signaling protein, *ESRRG* (estrogen related receptor gamma), was previously identified as a candidate gene for BKA.[22,23] *GREB1L* has been reported as a target of retinoic acid signaling, a pathway that is crucial for renal development and the dysregulation of which has been proposed as a causative mechanism for urinary tract malformations.[13,24–26] The recent identification of *GREB1L* mutations in two families with renal agenesis[27] highlighted this gene as a major actor of kidney differentiation.

In order to characterize the pattern of *GREB1L* expression, we first used cDNA panels from various human fetal and adult tissues. Analysis in fetal tissues showed major expression of *GREB1L* in the kidney (Figure 2A). Among adult tissues with the highest level of expression, we identified vagina, cervix, and epididymis (Figure 2B, see also Figure S2). Then, we analyzed in more detail *Greb1l* expression during kidney development using RNA *in situ* hybridization on frozen sections of wild-type mouse embryos and kidneys at different stages (Figures 2C–2F). Two antisense (AS) probes targeting different parts of *Greb1l* cDNA were synthesized. Staining with the control sense probes was negative and similar patterns of expression were observed with the two AS probes, validating their specificity. Sections of E16 mouse embryo showed a strong *Greb1l* expression in the liver, thymus, intestine, kidney, and brain (Figure 2C). The staining in the brain was particularly strong in the ventricular zone and in the neopallial cortex (the future cerebral cortex). In the kidney, at E16 all the stages of nephrogenesis are present. The strongest *Greb1l* staining was in the nephrogenic zone located in the cortical region of the kidney and identified by Six2 immunostaining performed in a serial section (Figure 2D).

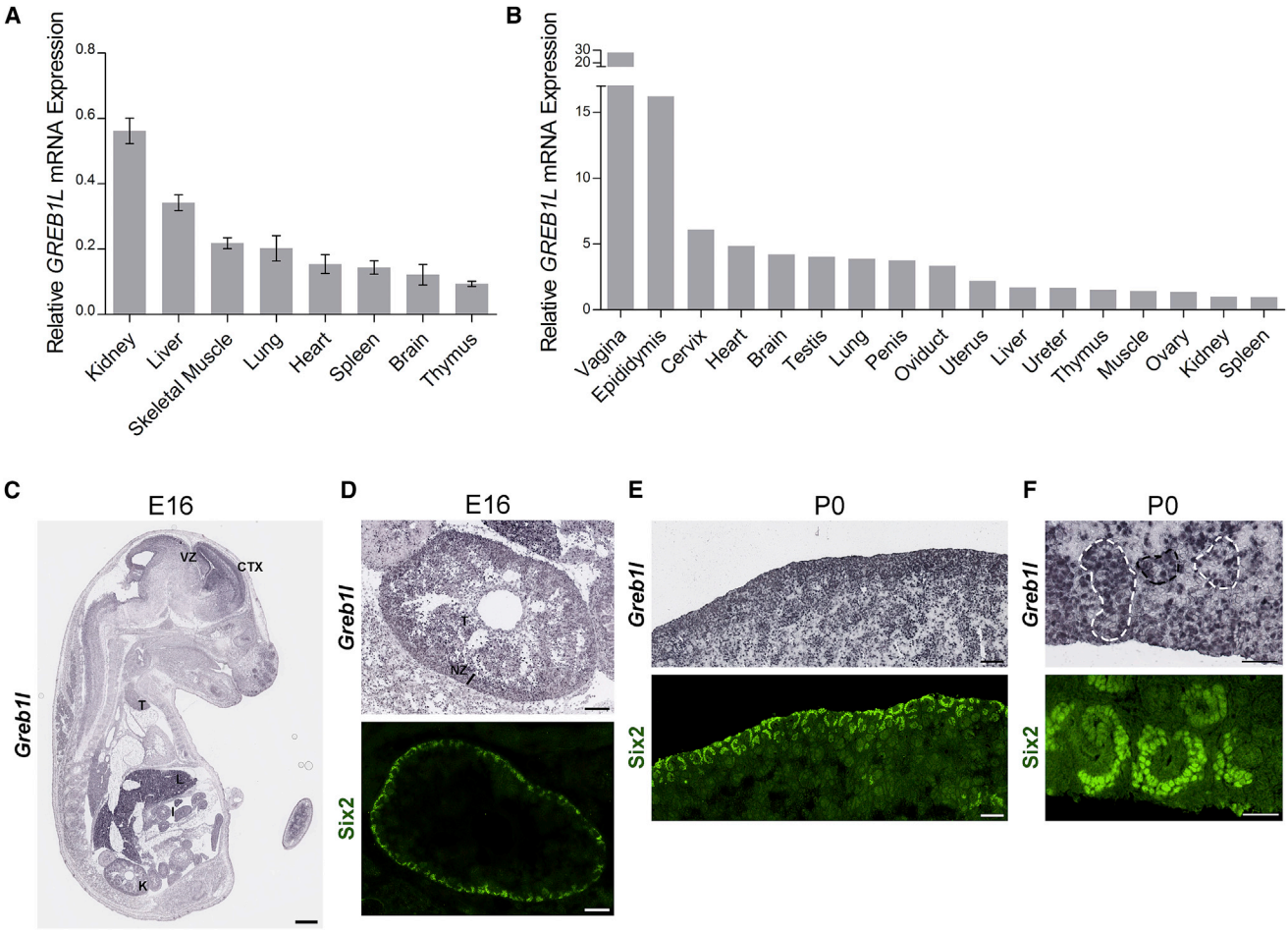

Figure 2. *GREB1L* Expression Pattern in Fetal and Adult Human Tissues and in Embryonic Mouse Kidney

(A) *GREB1L* mRNA expression levels in fetal human tissues were determined by quantitative real-time PCR using the Human Fetal MTC Panel (#636747, Clontech-Takara Bio Europe). *GREB1L* expression was normalized to the *GAPDH* expression and comparative Ct quantification was applied. Expression is displayed relative to the mRNA levels in the control cDNA provided by the kit. Error bar correspond to standard deviation (SD) of three independent experiments.

(B) *GREB1L* mRNA expression levels in human adult tissues was performed using the human major tissue qPCR panel that includes cDNAs from 48 normal tissues (#HMRT104, Origene). Quantification was performed according to the manufacturer's technical protocol. Expression is displayed relative to the mRNA level in the kidney. Results obtained with the complete panel are shown in Figure S2.

(C–F) Analysis of *Greb1l* expression during nephrogenesis by *in situ* hybridization in the mouse. Two *Greb1l* cDNA fragments were amplified by RT-PCR using mIMCD3 total RNA and subcloned into pGEMT-easy vector (Promega) for generation of RNA antisense probes, and sense probes as controls. Labeled RNA probes were synthesized with digoxigenin-11-UTP (Roche), according to the manufacturer's instructions. *In situ* hybridization in frozen sections of wild-type mouse embryos and kidneys was carried out as described.[38] In parallel immunostaining for Six2 (Proteintech, 1/200) was performed on serial sections.

(C) Section of E16 embryo stained with *Greb1l* RNA antisense probe AS-1. Abbreviations are as follows: L, liver; K, kidney; I, intestine; T, thymus; VZ, ventricular zone; CTX, future cerebral cortex. Scale bar, 1 mm.

(D) Zoom on the kidney from the E16 embryo showing *Greb1l* staining (top) and Six2 immunostaining (bottom). Abbreviations: NZ, nephrogenic zone; T, tubules. Scale bar, 200 μm.

(E and F) Kidney section at P0.

(E) Zoom on the nephrogenic zone showing *Greb1l* staining (top) and Six2 immunostaining (bottom). Scale bar, 200 μm.

(F) Image showing colocalization of *Greb1l* (top) and Six2 (bottom) in cap mesenchyme (surrounded in white) and a *Greb1l*-positive Six2-negative epithelial structure (surrounded in black). Scale bar, 50 μm.

Six2 is a marker of the cap mesenchyme, a multipotent nephron progenitor population intended to differentiate in epithelial nephronic structures in response to signals from the UB.[28] It thus allows identifying the region where the first steps of nephrogenesis occur. A widespread *Greb1l*-positive staining was also observed in epithelial cells of the differentiating, Six2-negative renal tubules. Strong *Greb1l* staining in the nephrogenic zone was confirmed in a kidney of a newborn pup at P0 (a stage where nephrogenesis is not finished in the mouse) (Figures 2E and 2F), where we clearly observed a partial colocalization with Six2 (Figure 2F, white outlined). *Greb1l* staining was also present in Six2-negative cells (Figure 2F, black outlined), indicating that *Greb1l* is also expressed in structures undergoing epithelial differentiation. This strongly suggests that *Greb1l* plays a role in the early steps of nephrogenesis.

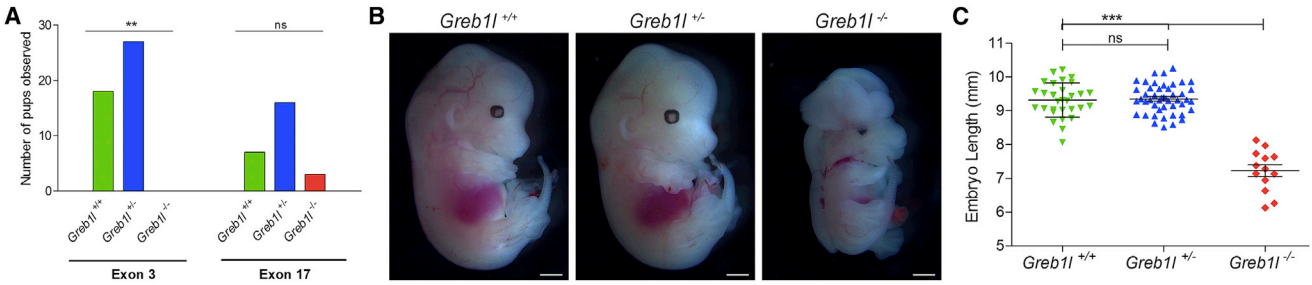

Figure 3. Analysis of the Offspring of *Greb1l* Mouse CRISPR-Cas9 Mutants

(A) Genotyping of the offspring of backcrosses and intercrosses described in Table S3B, showing embryonic lethality for *Greb1l*$^{-/-}$ embryos (homozygous or compound heterozygous frameshift mutations). Number of pups analyzed: 45 for exon 3 mutants and 26 for exon 17 mutants. The only 3 *Greb1l*$^{-/-}$ pups obtained (in red) were compound heterozygous with one of the mutations being an in-frame 3 bp deletion in exon 17 (see Table S3B). Chi-square test of observed versus expected genotypes; statistical significance **$p = 0.0015$.

(B) Whole-mount E13.5 embryos (delATAG mutation) showing the reduced size of *Greb1l*$^{-/-}$ embryos and the exencephaly. Scale bar, 1 mm.

(C) Quantification of the length of E13.5 embryos. Number of analyzed embryos: 30 *Greb1*$^{+/+}$, 48 *Greb1l*$^{+/-}$, 13 *Greb1*$^{-/-}$. Statistical significance ***$p < 0.0001$ (one-way ANOVA and Newman-Keuls multiple comparison test). Error bar: SD.

We then generated a *Greb1l* knock-out mouse model using CRISPR-Cas9 technology. Mice were maintained in a pathogen-free environment and experiments were conducted in accordance with French Government policies ("Services Vétérinaires de la Santé et de la Production Animale, Ministère de l'Agriculture"). The project was approved by the departmental director of "Services Vétérinaires de la Préfecture de Police de Paris" and by the ethical committee of the Paris Descartes University. Co-injection of single guide RNAs (sgRNAs) targeting either exon 3 (first coding exon) or exon 17 (out of frame exon) and Cas9 protein was performed in 195 1-cell-stage C57BL/6J eggs. Mice carrying mosaic heterozygous indel modifications in exon 3 (n = 2) or exon 17 (n = 5) were obtained, with a total of 9 different mutations (Table S3A). For sgRNA targeting exon 3, all the 11 exonic off-targets were tested to ascertain absence of mutation. The sgRNA targeting exon 17 did not match any exonic off-targets. Founders were backcrossed or intercrossed to generate 13 litters (Table S3B). All male and female founders were fertile and genotyping of the offspring showed inheritance of all the mutations at the heterozygous state. However, no pups carrying homozygous or compound heterozygous frameshift indels were obtained, indicating embryonic lethality (Figure 3A). The only 3 pups with compound heterozygous indels were those carrying an in-frame 3 bp deletion in addition to a 5 bp deletion.

We focused on the mouse line carrying the 4 bp c.64_68delATAG deletion in exon 3 (allele *Greb1l-a* in Table S3, Figure S3A). Analysis of the mutation at the cDNA level showed absence of exon skipping and expression of the delATAG allele at similar level as the wild-type allele in kidneys from *Greb1l*$^{+/-}$ embryos (Figure S3B). At the protein level, this mutated allele is predicted to lead to a frameshift and the creation of a premature stop codon (p.Iso22Lysfs*39) (Figure S3C), resulting in loss of function of the protein. Due to the embryonic lethality and the high level of resorption of *Greb1l*$^{-/-}$ embryos in the late stages of pregnancy, all the analyses were performed at E13.5. We observed that all *Greb1l*$^{-/-}$ embryos were significantly smaller compared to the *Greb1l*$^{+/+}$ and *Greb1l*$^{+/-}$ littermates and presented with exencephaly (Figures 3B and 3C). The high level of *Greb1l* expression in the brain, observed by *in situ* hybridization (Figure 2C), suggests that this gene likely plays a role in regulation of signaling pathways during brain development. We then focused on analysis of the urogenital system. At E13.5, the UB emerging from the mesonephric duct (i.e., Wolffian duct) has started elongating and branching to form the ureter and collecting ducts, while nephronic differentiation is well engaged. Mesonephric tubules (a transient kidney structure) are still there, and Wolffian ducts (precursors of vas deferens in males) and Müllerian ducts (precursors of oviduct, uterus, and upper part of the vagina in females) are both present in male and female embryos. Dissection of the urogenital system revealed presence of two kidneys in all *Greb1l*$^{+/-}$ embryos (n = 27) and lack of kidneys in all *Greb1l*$^{-/-}$ embryos (n = 7). We then used the recently published three-dimensional visualization technique allowing immunofluorescence analysis of whole embryos after clearing with 3DISCO.[29] *Greb1l*$^{+/+}$, *Greb1l*$^{+/-}$, and *Greb1l*$^{-/-}$ embryos were immunostained for Six2 or Pax2. While Six2 is expressed in metanephric progenitors, Pax2 has a much wider expression pattern, being expressed during the development of both ductal and mesenchymal components of the urogenital system.[30] As shown in Figures 4A and 4B, Pax2 staining showed presence of mesonephric tubules (MT) and Wolffian ducts (WD), kidney (K), ureter (U), and Müllerian ducts (MD) in *Greb1l*$^{+/+}$ and *Greb1l*$^{+/-}$ embryos. In contrast, both Pax2 and Six2 staining showed absence of kidney in all studied *Greb1l*$^{-/-}$ embryos (n = 10) (Figures 4A, 4B, and S4). Pax2 immunostaining also showed absence of

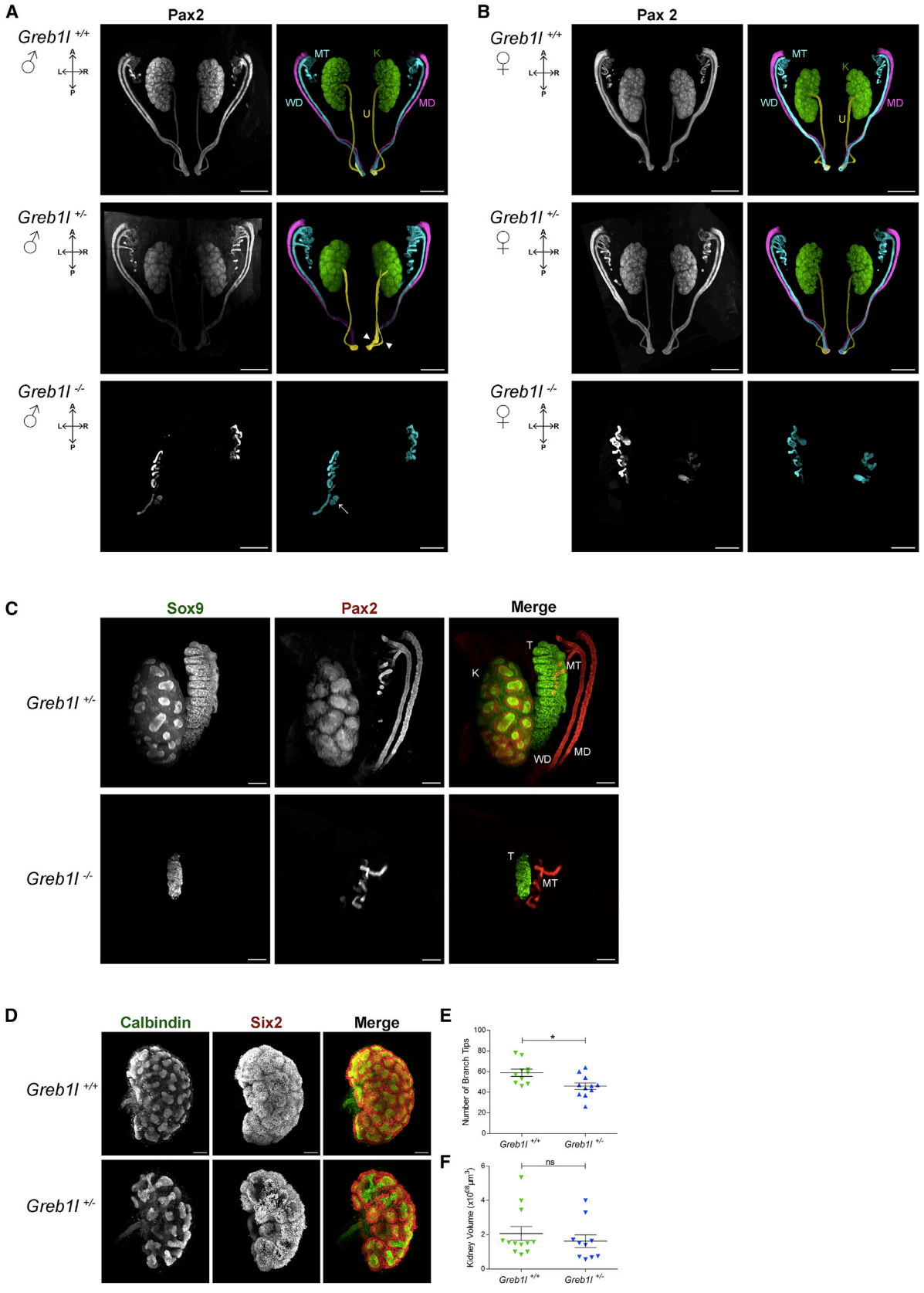

Figure 4. Characterization of *Greb1l*$^{-/-}$ and *Greb1l*$^{+/-}$ Kidney and Genital Tract Phenotypes

(A–C) Whole-mount immunofluorescence of E13.5 embryos showing absence of kidneys and Wolffian and Müllerian ducts in male and female *Greb1l*$^{-/-}$ embryos and abnormal testes in male *Greb1l*$^{-/-}$ embryos. Embryos were sacrificed at E13.5 in ice-cold 1× PBS and fixed in 4% PFA for 24 hr. For immunostaining, samples were incubated with anti-Pax2 antibody (Covance, 1/500 or R&D System, 1/300) or

(legend continued on next page)

Wolffian and Müllerian ducts in male (n = 3) and female (n = 4) *Greb1l*$^{-/-}$ embryos (Figures 4A and 4B). Absence of kidney and genital tract has been reported in *Pax2*$^{-/-}$ mouse embryos.[31] However, although *Pax2*$^{-/-}$ embryos do not develop mesonephros either, mesonephric tubules were the only structure that was consistently observed in E13.5 *Greb1l*$^{-/-}$ embryos (Figures 4A and 4B, lower panels), suggesting that *Greb1l* does not regulate the differentiation of the mesonephros. In addition, some structures that could be interpreted as a remnant of UB were present in most *Greb1l*$^{-/-}$ embryos (Figures 4A and 4B, lower panels, arrow), suggesting that UB had emerged from the Wolffian duct before it degenerates. Then, as mesonephric tubules and Wolffian duct are intended to form the drainage system of the testis, we sought to analyze whether testis formation was also altered in *Greb1l*$^{-/-}$ embryos using Sox9 immunostaining.[32] This showed that the gonads of the *Greb1l*$^{-/-}$ male embryos were severely affected, being small and with poorly organized sex-cords compared to *Greb1l*$^{+/-}$ embryos (Figure 4C). These data clearly demonstrate that *Greb1l* plays a major role in early steps of both metanephros and genital development.

Although analysis of *Greb1l*$^{+/-}$ embryos showed presence of normal sized kidneys in all studied embryos (n = 13), we observed a unilateral double ureter in one male embryo (Figure 4A, middle panel, arrowheads), suggesting that some *Greb1l*$^{+/-}$ embryos might present a mild CAKUT phenotype. Kidneys dissected from E13.5 *Greb1l*$^{+/+}$ (n = 6) and *Greb1l*$^{+/-}$ embryos (n = 8) were immunostained for Calbindin-D28K and Six2 in order to visualize UB tips and quantify branching. Light-sheet imaging of cleared kidneys[33] revealed a slight difference in branching in *Greb1l*$^{+/-}$ compared to *Greb1l*$^{+/+}$ embryos, although the volume of the kidneys was not significantly decreased (Figures 4D–4F). *RET*, a crucial regulator of UB branching, has been reported as a target of retinoic acid signaling.[24] Whether *Greb1l* plays a role in regulation of this gene will need to be established.

Finally, phenotypic analysis of the mutant mice was performed using micro computed tomography (microCT)[34] in order to look for alterations in other organs. The exencephaly and the lack of kidneys in *Greb1l*$^{-/-}$ were confirmed. In addition, a cardiac morphogenesis defect was identified in all *Greb1l*$^{-/-}$ embryos analyzed with this technique (n = 8) (Figure S5). Instead of the normal left-right position (Figure S5, upper and middle panels), the ventricles were both on the left and rotated by almost 90°, resulting in superimposed ventricles (Figure S5, lower panel). This phenotype is reminiscent of topsy-turvy heart.[35] Despite misorientation of these structures, the atria and the great vessels were seemingly well formed. All the other organs (lung, liver, intestine, stomach) appear to be normal and well positioned, although slightly underdeveloped. No anomaly was identified in the *Greb1l*$^{+/-}$ embryos (n = 9).

The phenotype of the mouse model thus recapitulates the kidney and uterus agenesis defects presented by *GREB1L* mutated human fetuses. As observed for other genes mutated in CAKUT,[5] the status of the mutations leading to these developmental defects is different in both species: heterozygous (with a maternal bias in transmission) in human, versus homozygous in the mouse. Presence of genital development defects in male *Greb1l*$^{-/-}$ mouse embryos suggests that heterozygous human mutations could lead to a reduced fertility in male individuals that could explain the maternal bias in transmission observed in the families. Heart defect and exencephaly were also consistently observed in *Greb1l*$^{-/-}$ mice. While heart defects were reported in two fetuses with *GREB1L* mutation, exencephaly was not observed in any of the fetuses, suggesting that heterozygous mutations may not be sufficient to cause this defect in human.

Finally, in order to further characterize the role of GREB1L in cellular mechanisms relevant for kidney formation, we analyzed its role in tubulomorphogenesis using murine inner medullary collecting duct (mIMCD3) cells

anti-Sox9 antibody (Millipore, 1/1,000) diluted in PBSGT (1× PBS, 0.2% gelatin, 0.5% Triton) + 0.1% Saponin (10 μg/mL) for 7 days at 37°C, then with secondary antibodies (donkey anti-rabbit IgG [H+L], Alexa Fluor 567, or donkey anti-goat IgG [H+L], Alexa Fluor 555) overnight at 37°C. Immunostaining and clearing with 3DISCO was performed as previously described.[29] Images were acquired with lightsheet ultramicroscope I (LaVision BioTec) using the ImspectorPro software (LaVision BioTec) and processed with Imaris x64 software.

(A and B) Pax2 staining was segmented and pseudo-colored to mark the different parts of the urogenital system. Kidneys are in green, ureters in yellow, Müllerian ducts in magenta, Wolffian ducts and mesonephric tubules in cyan. Scale bar, 300 μm. Shown are males (A) and females (B).

(C) Sox9 and Pax2 co-immunostaining in *Greb1l*$^{+/-}$ and *Greb1l*$^{-/-}$ male embryos showing abnormal testis (T) and absence of Wolffian and Müllerian ducts in *Greb1l*$^{-/-}$ embryo. Scale bar, 100 μm.

(D) Whole-mount immunofluorescence of kidneys from E13.5 *Greb1l*$^{+/+}$ and *Greb1l*$^{+/-}$ embryos. Embryos were dissected in ice-cold PBS and fixed in 4% PFA for 1 hr. Whole kidneys were blocked and permeabilized in 3% BSA, 0.075% Saponin, 0.1 M Na_4Cl, 1× PBS for 1 hr at room temperature. Samples were incubated with anti-Calbindin-D28K (Sigma-Aldrich, 1:3,000) and anti-Six2 (Proteintech, 1:400) overnight at 4°C, then with secondary antibodies (donkey anti-mouse IgG [H+L], Alexa Fluor 488 and donkey anti-rabbit IgG [H+L], Alexa Fluor 555) overnight at 4°C. Clearing was performed with Clear^{T2} as previously described.[33] Images were acquired with lightsheet microscope (Zeiss Z1, objective 20×). Scale bars, 100 μm.

(E) Ureteric bud branching was quantified considering Calbindin-D28K staining in *Greb1l*$^{+/+}$ and *Greb1l*$^{+/-}$ embryonic kidneys in a semiautomatic manner using Imaris x64 (v8.4.1). Number of samples: 10 *Greb1l*$^{+/+}$ and 11 *Greb1l*$^{+/-}$ kidneys. Statistical test: t test, *$p < 0.05$. Error bar: SEM.

(F) Volume of the kidneys was quantified with Imaris, using the manual "surface" tool, considering Six2 staining. Number of samples: 12 *Greb1l*$^{+/+}$ and 10 *Greb1l*$^{+/-}$ kidneys. Statistic t test was applied, error bar: SEM.

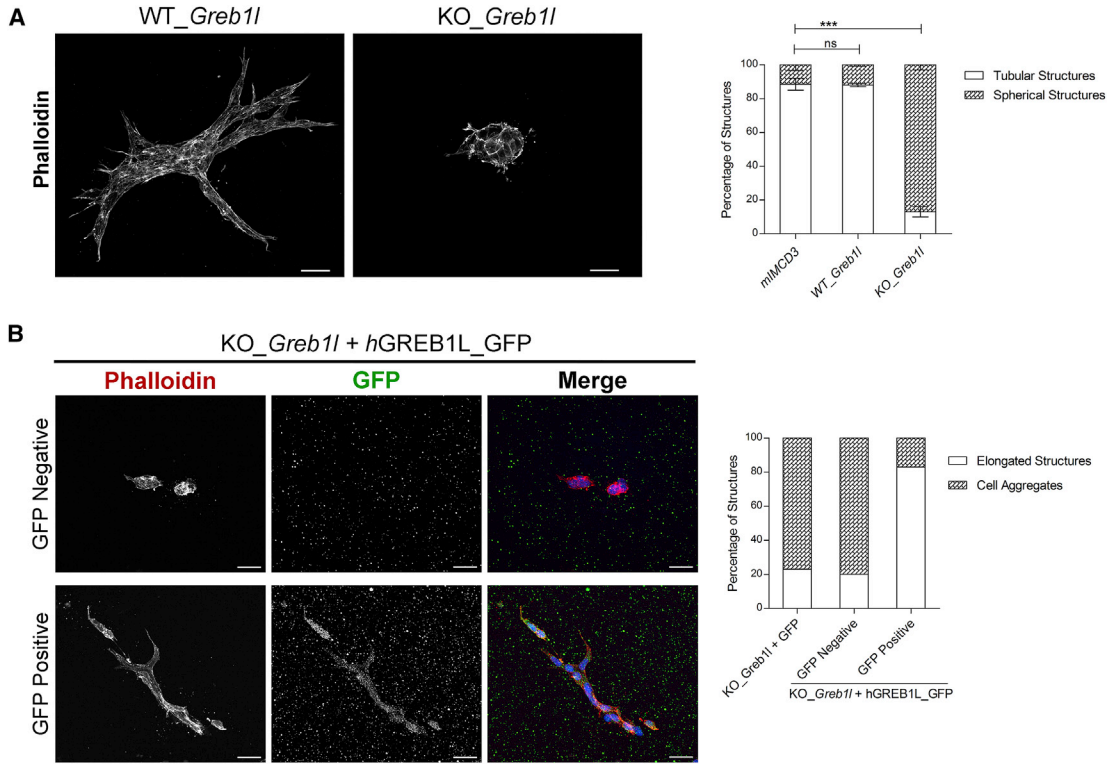

Figure 5. Tubulomorphogenesis Assay in *Greb1l* Knock-out mIMCD3 Cells

CRISPR-Cas9 technique was used for the generation of a *Greb1l* knock-out mIMCD3 cell line. The same sgRNA targeting exon 3 used for the mouse model was cloned in pSpCas9(BB)-2A-GFP (PX458), a gift from Feng Zhang (Addgene plasmid # 48138).[39] mIMCD3 cells were transfected with Lipofectamine 2000 Transfection Reagent (Invitrogen) and FACS sorted for GFP and single clones were selected and genotyped (see Figure S3D).

(A) Tubulomorphogenesis assay. KO_*Greb1l* and control WT_*Greb1l* clonal cells were cultured in a 46% collagen type I from rat tail (Corning) gel in 48-well plates. For each assay, each cell line was plated in 6 replicate wells. After 8 days of culture, cells were fixed in 4% PFA and immunostained with Alexa Fluor 555 Phalloidin (dilution 1/200) and structures were observed. Confocal images (Zeiss LSM 700) of representative structures are shown. For quantification, 200 structures were counted for each cell line in each experiment ($n = 2$). One-way ANOVA followed by Newman-Keuls multiple comparison test was applied: ***$p < 0.001$. Error bar: SEM.

(B) KO_*Greb1l* cells were transiently transfected either with *GREB1L* full-length cDNA fused with GFP or with empty GFP plasmid as a control, using Lipofectamine 2000. Cells were plated in 46% collagen I-rich gel 12 hr after transfection and cultured for 5 days in 6 replicate wells. Cells were fixed in PFA and immunostained with anti-GFP antibody and Alexa Fluor 555 Phalloidin. Confocal images of representative structures are shown. For quantification, 30 GFP-positive and 30 GFP-negative structures (KO_*Greb1l* + hGREB1L_GFP) and 60 stuctures (KO_*Greb1l* + GFP) were counted.

in 3D collagen I culture.[36] A *Greb1l* knock-out cellular model was generated by CRISPR-Cas9 using the same sgRNA targeting exon 3 as for the generation of the mouse model. Monoclonal cell populations were isolated and clones with homozygous indels were identified. We selected a clone with a homozygous deletion of 26 bp (KO_*Greb1l*, Figure S3D) for subsequent analyses. As a control, we used a clone in which no mutational event in *Greb1l* was identified (WT_*Greb1l*, Figure S3D). All the 11 exonic off-targets were tested to ascertain absence of mutation. After 8 days of culture in collagen I gel, both the WT_*Greb1l* cells and the mIMCD3 polyclonal cell line were able to form tubule-like structures (Figure 5A). In contrast, KO_*Greb1l* cells failed to form tubules and grew as small spherical structures. This phenotype was rescued by transient transfection of a GFP-fused human *GREB1L* construct. After 5 days of culture, we observed that the transfected, GFP-positive cells mostly formed elongated structures modeling the first step of tubulomorphogenesis, whereas the GFP-negative cells grew in sphere aggregates similarly to the control cells transfected with empty vector (Figure 5B). This demonstrates that GREB1L is involved in tubulogenesis. This result is coherent with those from Simandi et al. that suggested the role of GREB1L in cell differentiation.[25]

In conclusion, we report here the identification of *GREB1L* as a gene whose mutations lead to CAKUT. We formally demonstrate that heterozygous *GREB1L* loss-of-function mutations in humans cause BKA, a phenotype also displayed by *Greb1l*$^{-/-}$ mice. Although we did not functionally validate the effect of the missense variants, enrichment in such variants in CAKUT-affected case subjects, significant association with BKA, maternal bias in transmission (also observed for loss-of-function mutations), as well as the *de novo* occurrence of one of the missense variants, are convergent elements supporting the likely pathogenicity of these variants. Our results present evidence that *Greb1l* plays a role in early kidney

differentiation as well as in genital tract development in mice and provide a genetic cause for the association of female genital tract defects and CAKUT in human, an association that is frequent but rarely explained.[37] Further studies will be necessary to decipher the pathways that are regulated by *GREB1L* and crosstalks with known genitourinary developmental mechanisms.

Supplemental Data

Supplemental Data include five figures and three tables and can be found with this article online at https://doi.org/10.1016/j.ajhg.2017.09.026.

Acknowledgments

We thank affected individuals and families for their participation. We also thank the foetopathologists of the SOciété Française de FOETopatholgie (SOFFOET) for providing us with fetal tissue samples, and the pediatric nephrologists from the French Society of Pediatric Nephrology and geneticists for referring the patients. We specifically thank Drs. Dominique Gaillard and Martine Doco. We are very grateful to Yuliya Petrov and Anrifati Harouna for providing us with family 5 grandparents' DNAs. We thank Drs. Lorrie le Page and Nicole Joyé for providing us with clinical information for some of the families. We warmly thank Marie-Claire Gubler for her precious help with histology analysis of fetal kidneys as well as Brigitte Lelongt for her help in dissection of mouse embryos. We are grateful to Sophie Berissi and Sophie Bernard (Small Animal Histology and Morphology platform, Necker) for tissue sections and slide scans. We acknowledge Meriem Garfa-Traoré and Nicolas Goudin (Necker Cell Imaging Platform), Emilie Panafieu, Laëtitia Duhamel, Alexandra Levostre, Yann Zimmermann, and Cristian Dicu (LEAT, Animal facility) and Lotfi Slimani and Jérémy Sadoine (Platform Imagerie du Vivant, Université Paris Descartes) for their excellent technical assistance. We are also grateful to Marion Delous who introduced us to the embryo clearing technique. The research leading to these results has received funding from the European Union's Seventh Framework Programme (FP7/2007–2013) grant 305608 (EURenOmics). C.H. was funded by EURenOmics. This work was also supported by GIS-Institut des Maladies Rares (AMA11025KSA to C.J.), Fondation pour la Recherche Médicale (DEQ20130326532 to S.S.), and state funding from the Agence Nationale de la Recherche under "Investissements d'avenir" program (ANR-10-IAHU-01 to S.S.).

Received: July 10, 2017
Accepted: September 28, 2017
Published: November 2, 2017

Web Resources

CADD, http://cadd.gs.washington.edu/
Combined and Multivariate Collapsing Method for Rare Variants, http://varianttools.sourceforge.net/Association/CMC
CRISPOR, http://crispor.tefor.net/
Emouseatlas, http://www.emouseatlas.org/emap/home.html
Ensembl Genome Browser, http://www.ensembl.org/index.html
GenBank, https://www.ncbi.nlm.nih.gov/genbank/
GeneCards, http://www.genecards.org
GenitoUrinary Molecular Anatomy Project (GUDMAP), http://www.gudmap.org/
gnomAD Browser, http://gnomad.broadinstitute.org/
Mouse Genome Informatics, http://www.informatics.jax.org/
OMIM, http://www.omim.org/
PolyPhen-2, http://genetics.bwh.harvard.edu/pph2/
SIFT, http://sift.bii.a-star.edu.sg/
UniProt, http://www.uniprot.org/

References

1. Loane, M., Dolk, H., Kelly, A., Teljeur, C., Greenlees, R., Densem, J.; and EUROCAT Working Group (2011). Paper 4: EUROCAT statistical monitoring: identification and investigation of ten year trends of congenital anomalies in Europe. Birth Defects Res. A Clin. Mol. Teratol. *91* (*Suppl 1*), S31–S43.
2. Ardissino, G., Daccò, V., Testa, S., Bonaudo, R., Claris-Appiani, A., Taioli, E., Marra, G., Edefonti, A., Sereni, F.; and ItalKid Project (2003). Epidemiology of chronic renal failure in children: data from the ItalKid project. Pediatrics *111*, e382–e387.
3. Schedl, A. (2007). Renal abnormalities and their developmental origin. Nat. Rev. Genet. *8*, 791–802.
4. Little, M.H., and McMahon, A.P. (2012). Mammalian kidney development: principles, progress, and projections. Cold Spring Harb. Perspect. Biol. *4*, 4.
5. Heidet, L., Morinière, V., Henry, C., De Tomasi, L., Reilly, M.L., Humbert, C., Alibeu, O., Fourrage, C., Bole-Feysot, C., Nitschké, P., et al. (2017). Targeted exome sequencing identifies PBX1 as involved in monogenic congenital anomalies of the kidney and urinary tract. J. Am. Soc. Nephrol. *28*, 2901–2914.
6. Uy, N., and Reidy, K. (2016). Developmental genetics and congenital anomalies of the kidney and urinary tract. J. Pediatr. Genet. *5*, 51–60.
7. Vivante, A., Kohl, S., Hwang, D.Y., Dworschak, G.C., and Hildebrandt, F. (2014). Single-gene causes of congenital anomalies of the kidney and urinary tract (CAKUT) in humans. Pediatr. Nephrol. *29*, 695–704.
8. Barak, H., Huh, S.H., Chen, S., Jeanpierre, C., Martinovic, J., Parisot, M., Bole-Feysot, C., Nitschké, P., Salomon, R., Antignac, C., et al. (2012). FGF9 and FGF20 maintain the stemness of nephron progenitors in mice and man. Dev. Cell *22*, 1191–1207.
9. Humbert, C., Silbermann, F., Morar, B., Parisot, M., Zarhrate, M., Masson, C., Tores, F., Blanchet, P., Perez, M.J., Petrov, Y., et al. (2014). Integrin alpha 8 recessive mutations are responsible for bilateral renal agenesis in humans. Am. J. Hum. Genet. *94*, 288–294.
10. Jeanpierre, C., Macé, G., Parisot, M., Morinière, V., Pawtowsky, A., Benabou, M., Martinovic, J., Amiel, J., Attié-Bitach, T., Delezoide, A.L., et al.; Société Française de Foetopathologie (2011). RET and GDNF mutations are rare in fetuses with renal agenesis or other severe kidney development defects. J. Med. Genet. *48*, 497–504.
11. Skinner, M.A., Safford, S.D., Reeves, J.G., Jackson, M.E., and Freemerman, A.J. (2008). Renal aplasia in humans is associated with RET mutations. Am. J. Hum. Genet. *82*, 344–351.
12. van Haelst, M.M., Maiburg, M., Baujat, G., Jadeja, S., Monti, E., Bland, E., Pearce, K., Hennekam, R.C., Scambler, P.J.; and Fraser Syndrome Collaboration Group (2008). Molecular study of 33 families with Fraser syndrome new data and mutation review. Am. J. Med. Genet. A. *146A*, 2252–2257.

13. Ochsner, S.A., Watkins, C.M., McOwiti, A., Xu, X., Darlington, Y.F., Dehart, M.D., Cooney, A.J., Steffen, D.L., Becnel, L.B., and McKenna, N.J. (2012). Transcriptomine, a web resource for nuclear receptor signaling transcriptomes. Physiol. Genomics *44*, 853–863.
14. Kanwar, Y.S., Pan, X., Lin, S., Kumar, A., Wada, J., Haas, C.S., Liau, G., and Lomasney, J.W. (2003). Imprinted mesodermal specific transcript (MEST) and H19 genes in renal development and diabetes. Kidney Int. *63*, 1658–1670.
15. Dekel, B., Metsuyanim, S., Schmidt-Ott, K.M., Fridman, E., Jacob-Hirsch, J., Simon, A., Pinthus, J., Mor, Y., Barasch, J., Amariglio, N., et al. (2006). Multiple imprinted and stemness genes provide a link between normal and tumor progenitor cells of the developing human kidney. Cancer Res. *66*, 6040–6049.
16. Garne, E., Loane, M., Dolk, H., Barisic, I., Addor, M.C., Arriola, L., Bakker, M., Calzolari, E., Matias Dias, C., Doray, B., et al. (2012). Spectrum of congenital anomalies in pregnancies with pregestational diabetes. Birth Defects Res. A Clin. Mol. Teratol. *94*, 134–140.
17. Vivante, A., Hwang, D.Y., Kohl, S., Chen, J., Shril, S., Schulz, J., van der Ven, A., Daouk, G., Soliman, N.A., Kumar, A.S., et al. (2017). Exome sequencing discerns syndromes in patients from consanguineous families with congenital anomalies of the kidneys and urinary tract. J. Am. Soc. Nephrol. *28*, 69–75.
18. San Lucas, F.A., Wang, G., Scheet, P., and Peng, B. (2012). Integrated annotation and analysis of genetic variants from next-generation sequencing studies with variant tools. Bioinformatics *28*, 421–422.
19. Wang, G.T., Peng, B., and Leal, S.M. (2014). Variant association tools for quality control and analysis of large-scale sequence and genotyping array data. Am. J. Hum. Genet. *94*, 770–783.
20. Li, B., and Leal, S.M. (2008). Methods for detecting associations with rare variants for common diseases: application to analysis of sequence data. Am. J. Hum. Genet. *83*, 311–321.
21. Deschênes, J., Bourdeau, V., White, J.H., and Mader, S. (2007). Regulation of GREB1 transcription by estrogen receptor alpha through a multipartite enhancer spread over 20 kb of upstream flanking sequences. J. Biol. Chem. *282*, 17335–17339.
22. Harewood, L., Liu, M., Keeling, J., Howatson, A., Whiteford, M., Branney, P., Evans, M., Fantes, J., and Fitzpatrick, D.R. (2010). Bilateral renal agenesis/hypoplasia/dysplasia (BRAHD): postmortem analysis of 45 cases with breakpoint mapping of two de novo translocations. PLoS ONE *5*, e12375.
23. Berry, R., Harewood, L., Pei, L., Fisher, M., Brownstein, D., Ross, A., Alaynick, W.A., Moss, J., Hastie, N.D., Hohenstein, P., et al. (2011). Esrrg functions in early branch generation of the ureteric bud and is essential for normal development of the renal papilla. Hum. Mol. Genet. *20*, 917–926.
24. Rosselot, C., Spraggon, L., Chia, I., Batourina, E., Riccio, P., Lu, B., Niederreither, K., Dolle, P., Duester, G., Chambon, P., et al. (2010). Non-cell-autonomous retinoid signaling is crucial for renal development. Development *137*, 283–292.
25. Simandi, Z., Horvath, A., Wright, L.C., Cuaranta-Monroy, I., De Luca, I., Karolyi, K., Sauer, S., Deleuze, J.F., Gudas, L.J., Cowley, S.M., and Nagy, L. (2016). OCT4 acts as an integrator of pluripotency and signal-induced differentiation. Mol. Cell *63*, 647–661.
26. Vivante, A., Mann, N., Yonath, H., Weiss, A.C., Getwan, M., Kaminski, M.M., Bohnenpoll, T., Teyssier, C., Chen, J., Shril, S., et al. (2017). A dominant mutation in nuclear receptor interacting protein 1 causes urinary tract malformations via dysregulation of retinoic acid signaling. J. Am. Soc. Nephrol. *28*, 2364–2376.
27. Brophy, P.D., Rasmussen, M., Parida, M., Bonde, G., Darbro, B.W., Hong, X., Clarke, J.C., Peterson, K.A., Denegre, J., Schneider, M., et al. (2017). A gene implicated in activation of retinoic acid receptor targets is a novel renal agenesis gene in humans. Genetics *207*, 215–228.
28. Kobayashi, A., Valerius, M.T., Mugford, J.W., Carroll, T.J., Self, M., Oliver, G., and McMahon, A.P. (2008). Six2 defines and regulates a multipotent self-renewing nephron progenitor population throughout mammalian kidney development. Cell Stem Cell *3*, 169–181.
29. Belle, M., Godefroy, D., Couly, G., Malone, S.A., Collier, F., Giacobini, P., and Chédotal, A. (2017). Tridimensional visualization and analysis of early human development. Cell *169*, 161–173.e12.
30. Dressler, G.R., Deutsch, U., Chowdhury, K., Nornes, H.O., and Gruss, P. (1990). Pax2, a new murine paired-box-containing gene and its expression in the developing excretory system. Development *109*, 787–795.
31. Torres, M., Gómez-Pardo, E., Dressler, G.R., and Gruss, P. (1995). Pax-2 controls multiple steps of urogenital development. Development *121*, 4057–4065.
32. Chaboissier, M.C., Kobayashi, A., Vidal, V.I., Lützkendorf, S., van de Kant, H.J., Wegner, M., de Rooij, D.G., Behringer, R.R., and Schedl, A. (2004). Functional analysis of Sox8 and Sox9 during sex determination in the mouse. Development *131*, 1891–1901.
33. Kuwajima, T., Sitko, A.A., Bhansali, P., Jurgens, C., Guido, W., and Mason, C. (2013). ClearT: a detergent- and solvent-free clearing method for neuronal and non-neuronal tissue. Development *140*, 1364–1368.
34. Degenhardt, K., Wright, A.C., Horng, D., Padmanabhan, A., and Epstein, J.A. (2010). Rapid 3D phenotyping of cardiovascular development in mouse embryos by micro-CT with iodine staining. Circ Cardiovasc Imaging *3*, 314–322.
35. Güzeltaş, A., Öztürk, E., and Diker, M. (2013). Topsy-turvy heart: a very rare case of superoinferior ventricle. Pediatr. Cardiol. *34*, 2096–2098.
36. Mai, W., Chen, D., Ding, T., Kim, I., Park, S., Cho, S.Y., Chu, J.S., Liang, D., Wang, N., Wu, D., et al. (2005). Inhibition of Pkhd1 impairs tubulomorphogenesis of cultured IMCD cells. Mol. Biol. Cell *16*, 4398–4409.
37. Oram, R.A., Edghill, E.L., Blackman, J., Taylor, M.J., Kay, T., Flanagan, S.E., Ismail-Pratt, I., Creighton, S.M., Ellard, S., Hattersley, A.T., and Bingham, C. (2010). Mutations in the hepatocyte nuclear factor-1β (HNF1B) gene are common with combined uterine and renal malformations but are not found with isolated uterine malformations. Am. J. Obstet. Gynecol. *203*, 364.e1–364.e5.
38. Heidet, L., Cai, Y., Sado, Y., Ninomiya, Y., Thorner, P., Guicharnaud, L., Boye, E., Chauvet, V., Solal, L.C., Beziau, A., et al. (1997). Diffuse leiomyomatosis associated with X-linked Alport syndrome: extracellular matrix study using immunohistochemistry and in situ hybridization. Lab. Invest. *76*, 233–243.
39. Ran, F.A., Hsu, P.D., Wright, J., Agarwala, V., Scott, D.A., and Zhang, F. (2013). Genome engineering using the CRISPR-Cas9 system. Nat. Protoc. *8*, 2281–2308.

The American Journal of Human Genetics, Volume *101*

Supplemental Data

Mutations in *GREB1L* Cause Bilateral Kidney Agenesis in Humans and Mice

Lara De Tomasi, Pierre David, Camille Humbert, Flora Silbermann, Christelle Arrondel, Frédéric Tores, Stéphane Fouquet, Audrey Desgrange, Olivier Niel, Christine Bole-Feysot, Patrick Nitschké, Joëlle Roume, Marie-Pierre Cordier, Christine Pietrement, Bertrand Isidor, Philippe Khau Van Kien, Marie Gonzales, Marie-Hélène Saint-Frison, Jelena Martinovic, Robert Novo, Juliette Piard, Christelle Cabrol, Ishwar C. Verma, Ratna Puri, Hubert Journel, Jacqueline Aziza, Laurent Gavard, Marie-Hélène Said-Menthon, Laurence Heidet, Sophie Saunier, and Cécile Jeanpierre

Family 5: c.4607A>G; p.His1536Arg

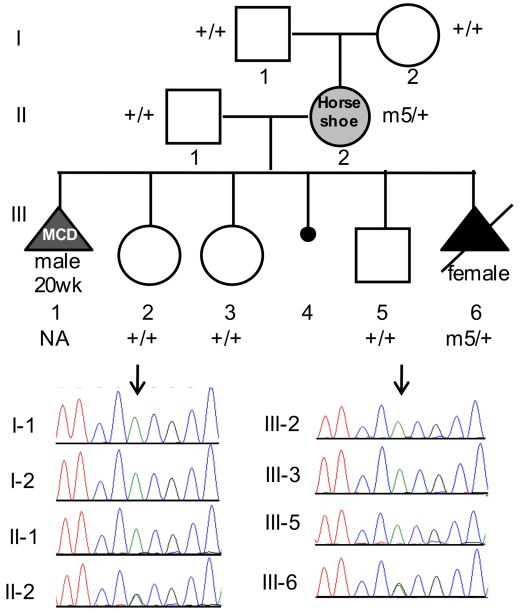

Family 6: c.4505T>C; p.Met1502Thr

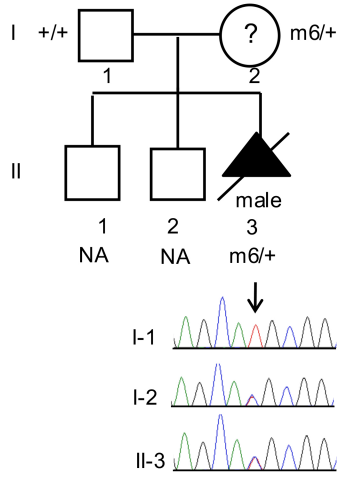

Family 7: c.4672C>A; p.Arg1558Ser

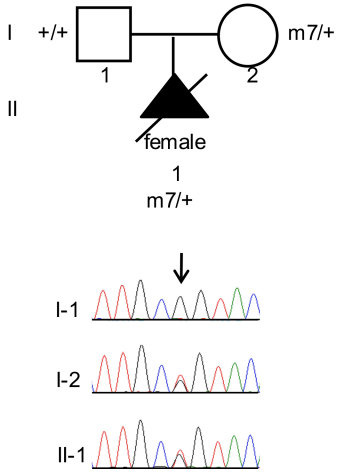

Family 8: c.2251C>T; p.Arg751Cys

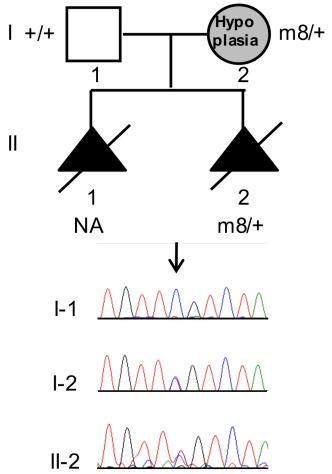

Family 9:c.575G>T; p.Arg192Leu

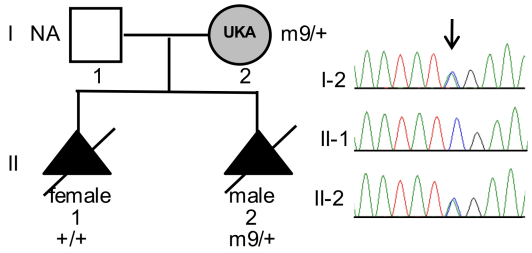

Family 10: c.4727C>T; p.Ala1576Val

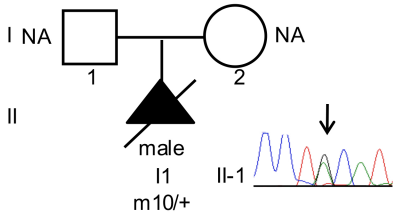

Family 11: c.4526A>T ; p.Asp1509Val

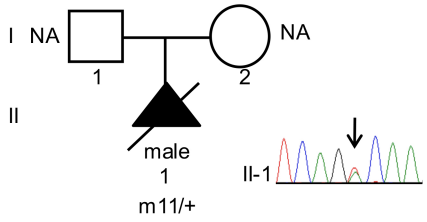

Family 12: c.5323 G>A; p.Asp1775Asn

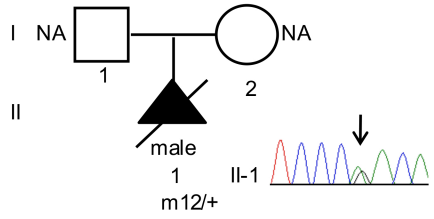

Family 13: c.2252 G>A; p.Arg751His

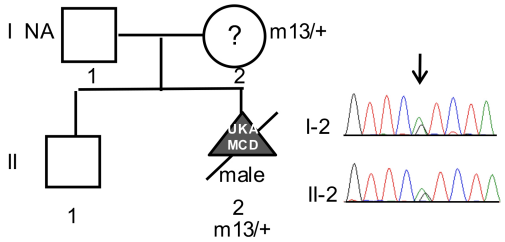

Family 14: c.983G>A; p.Arg328Gln

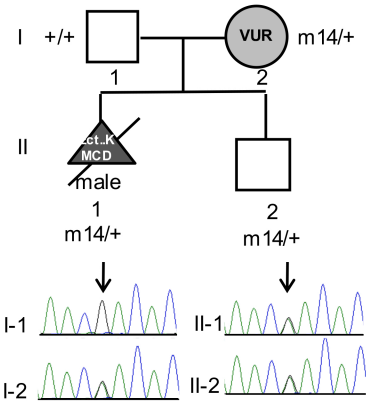

Family 15:c.1813A>C; p.Ser605Arg

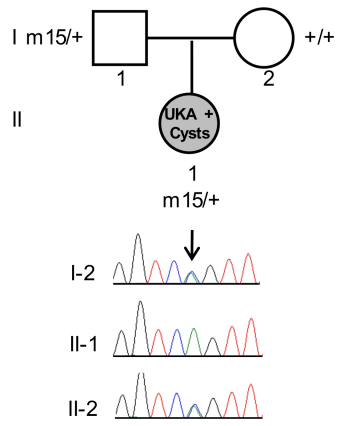

Family 16: c.2148 G>T; p.Leu716Phe

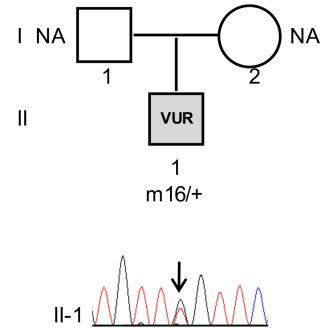

Figure S1. Identification of *Greb1l* heterozygous missense variants in 12 CAKUT families/cases

For each missense variant, the pedigree leading to variant identification and Sanger sequencing chromatograms are shown with the position of the mutations indicated by arrows.

In black: cases with bilateral kidney agenesis; in grey: cases with other indicated phenotypes (UKA = unilateral kidney agenesis; Ect. K = ectopic kidney; MCD = multicystic dysplasia; VUR = vesicoureteral reflux). Question marks mean that the renal status has not been ascertained by renal ultrasound.

NA = individual with non-available DNA.

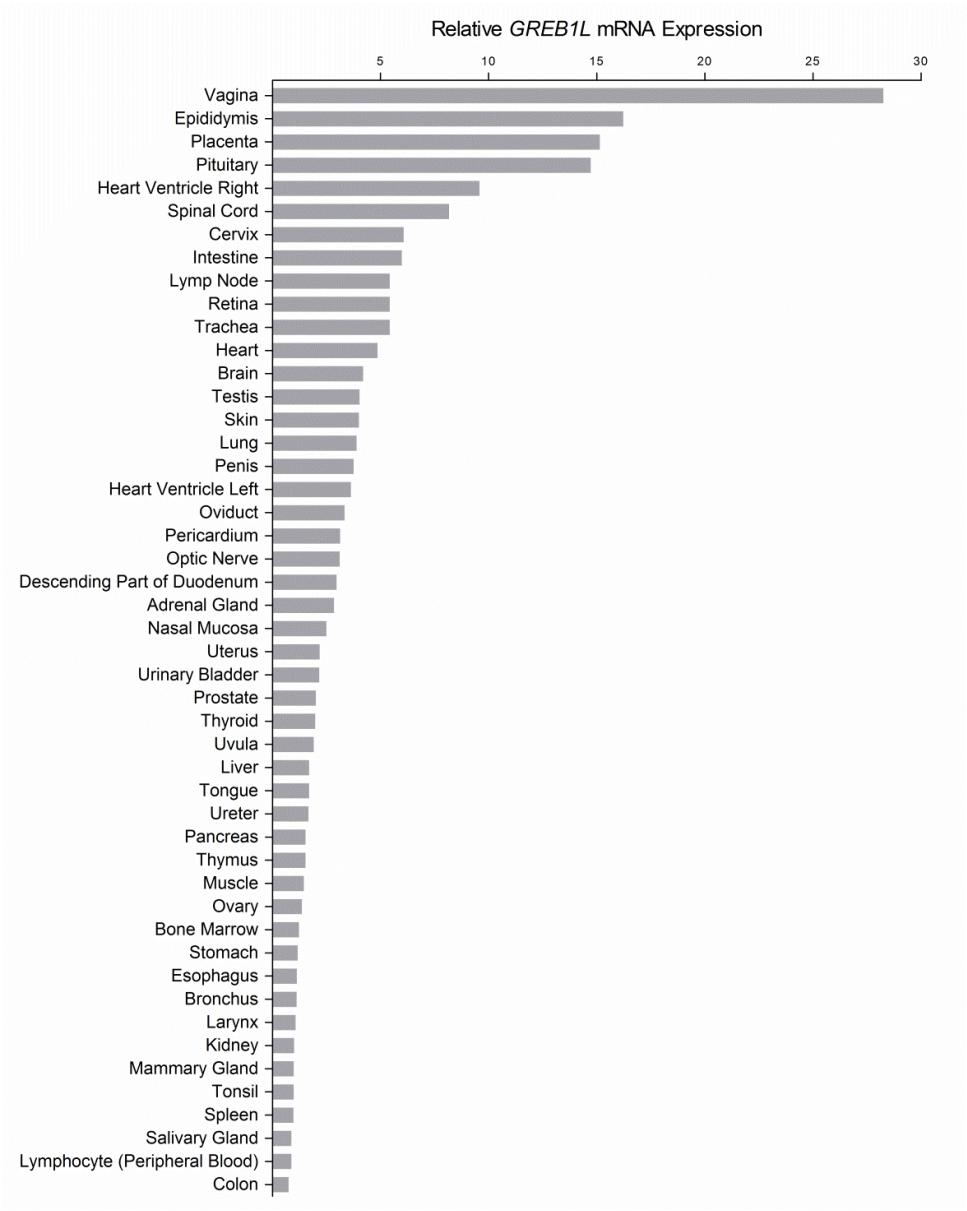

Figure S2: Quantification of the expression of *GREB1L* in 48 human tissues

GREB1L mRNA expression levels in adult human tissues were determined by quantitative Real-Time PCR using the Human Major Tissue qPCR panel (#HMRT104, Origene Technologies, Rockville, USA). Quantification was performed according to the manufacturer's instruction. Expression is displayed relative to the mRNA level in the kidney.

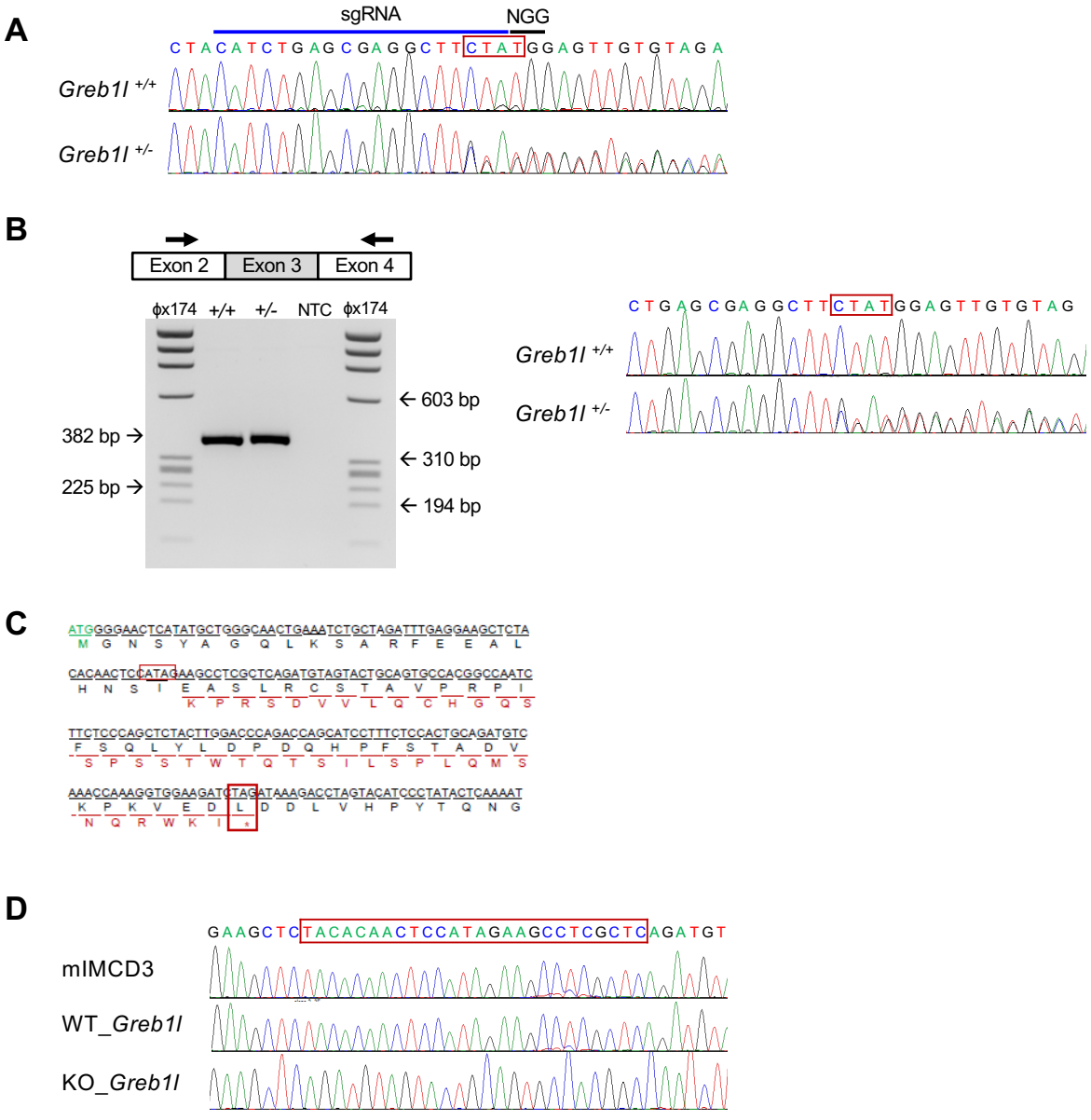

Figure S3: Identification of a four base pair deletion in *Greb1l* exon 3 (c.64_68delATAG) in a mouse mutant obtained by CRISPR-Cas9

(A) Genomic DNA extracted from tails of 10 days-old mice obtained after microinjection of a sgRNA targeting *Greb1l* exon 3 was sequenced using primers spanning exon 3, leading to the identification of a founder carrying a heterozygous ATAG deletion (red box). Sanger sequencing was performed using the reverse primer.

(B) PCR amplification of kidney cDNAs from *Greb1*$^{+/+}$ and *Greb1l*$^{+/-}$ E13.5 embryos showing a 382 bp fragment spanning exon 3 in both cases and absence of skipping of exon 3 in *Greb1*$^{+/-}$ cDNA. Primers (black arrows) were located in exon 2 and exon 4. Sanger sequencing of the 382 bp fragment demonstrating expression of the mutated allele at a similar level as the wild type allele in the kidney of E13.5 *Greb1l*$^{+/-}$ embryos. Sequencing was performed using the reverse primer.

(C) Protein sequence corresponding to the mutated allele showing the predicted premature stop codon.

(D) Sanger sequencing of *Greb1l* exon 3 in gDNA extracted from mIMCD3 cells and WT_*Greb1l* and KO_*Greb1l* clones, showing the c.53_79del (red box) in the KO_*Greb1l* clone.

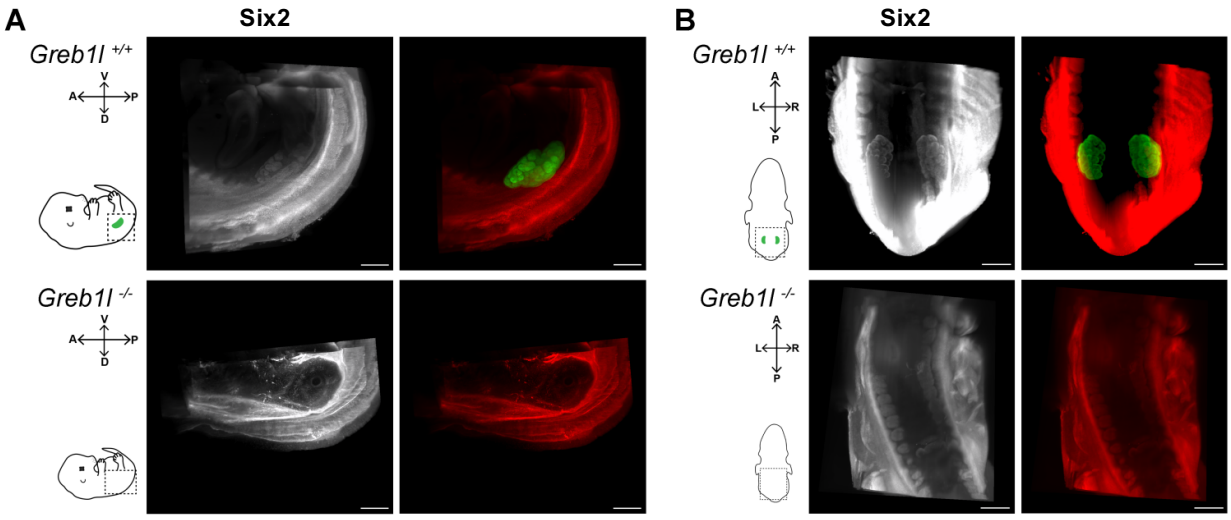

Figure S4. Characterization of *Greb1l*$^{-/-}$ and *Greb1l*$^{+/-}$ kidney phenotypes

Whole-mount immunofluorescence of E13.5 embryos after staining with anti-Six2 antibody (Proteintech, 1/200) and clearing with 3DISCO. Images were acquired with lightsheet ultramicroscope I (LaVision BioTec) and processed with Imaris x64 software. Due to the high level of Six2 external background, the specific kidney staining was isolated using the manual "surface" tool and pseudo-colored in green. 3D pictures were generated using the "snapshot" tool. Scale bar 300µm. (A) Lateral view. (B) Dorsal view.

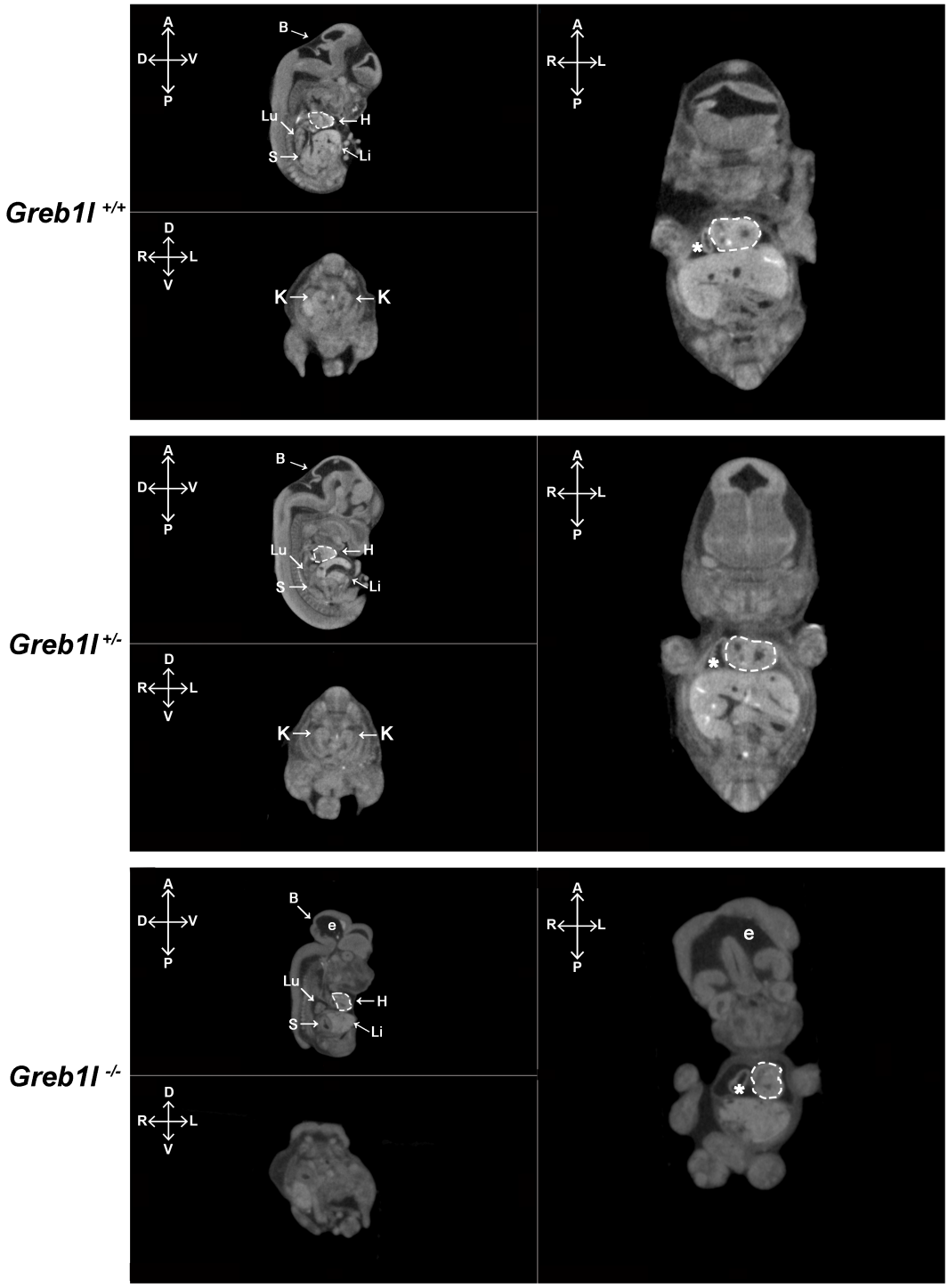

Figure S5: MicroCT analysis of embryos at E13.5 showing absence of kidneys, exencephaly and heart defects in *Greb1l* $^{-/-}$

Embryos were sacrificed at E13.5 in cold 250mM KCl, fixed in 4% PFA and incubated in Lugol solution for 24h before microCT scanning (Micro-CT Quantum FX). Lateral, transversal and frontal views of *Greb1l*$^{+/+}$ (upper panel), *Greb1l*$^{+/-}$ (middle panel) and *Greb1l*$^{-/-}$ (lower panel) embryos. The heart is outlined in white in the lateral and frontal views showing the superimposed ventricles in *Greb1l*$^{-/-}$. The atrium is identify by an asterisk. Lack of kidney is visible in the transversal view of *Greb1l*$^{-/-}$ embryos.

B = brain, Lu = lung, H = heart, S = stomach, Li = liver, K = kidney, e = exencephaly.

Table S1: Analysis of WES in families 1 and 2

Variants	Family 1 (common to 3 affected fetuses + child)	Family 2 (common to 2 affected fetuses)
Total number of variants	56000	91943
Total number of coding variants	16147	25439
Rare coding variants (not in in-house database, MAF <0.01%)	34	85
Rare coding variants (not in in-house database, MAF <0.01%) excluding synonymous	28	70
Variants in regions identified by linkage study (dominant model)	10	NA
Not in GnomAD	4	34
With deleterious effect (LOF + MS predicted to be damaging)	2	20
LOF	1	4
	GREB1L, NM_001142966.1:c.1582del, p.(Gln528Argfs*12)	*GREB1L,* NM_001142966.1:c.4369-1G>C *CPSF3L,* NM_001256456.1: c.673C>T, p.Arg225* *MYOM2,* NM_003970.3: c.153_156del, p.Ser52Leufs*23) *MCTP2,* NM_018349.3:c.292C>T, p.Gln98*)

MAF = minor allele frequency, based on public databases (dbSNP, EVS, 1000 genome, ExAC and GnomAD); LOF = loss-of-function; MS = missense; NA = not available

Whole exome sequencing was performed using the 50 Mb Agilent SureSelect all exon V3. Sequencing was performed on a HiSeq2500 (Illumina) sequencer. Sequence data were aligned to the human genome reference sequence (hg19 build) using BWA aligner. Downstream processing was carried out with the Genome Analysis Toolkit (GATK), SAMtools, and Picard (http://www.broadinstitute.org/gatk/guide/topic?name=best-practices). The average coverage was 86, with 93.5% of the targeted regions covered > 15X. Variants were annotated using a software system developed by the Paris Descartes University Bioinformatics Platform, based on the Ensembl (GRCh37/hg19), dbSNP, EVS, 1000 genome, ExAC and GnomAD databases. Variants were then prioritized according to their damaging effect (nonsense, frameshift, acceptor/donor splice site mutations, missense variants predicted to be damaging, and their absence in GnomAD and in our in-house database (> 10 000 exomes). For missense variants, prediction of damaging effect was based on PolyPhen2[1], Sift[2], Grantham[3] and CADD[4] scores. Prediction of the effect of variants on splicing were based on SpliceSiteFinder, MaxEntScan, NNSPLICE, GeneSplicer and HumanSplicingFinder through Alamut[5].

Table S2. Enrichment in rare damaging *GREB1L* variants in CAKUT cases

num_variants_ FisherMidP	statistic_ FisherMidP	pvalue_ FisherMidP
CAKUT (n = 183) versus controls (n=361): LOF + MS		
18	5.89822	0.0001935
CAKUT (n = 183) versus controls (n=361): MS		
14	4.11561	0.00501263
CAKUT BKA (n=54) versus non BKA (n=129) LOF + MS		
14	10.7442	6.05569E-05
CAKUT BKA (n=54) versus non BKA (n=129) MS		
10	6.25532	0.00445344

Comparison of the number of rare loss-of-function and damaging missense variants in cases versus controls using Combined and Multivariate Collapsing (CMC) test.

LOF = loss-of-function (nonsense, frameshift and splice acceptor/donor variants);

MS = missense variants, predicted as (i) probably / possibly damaging with Polyphen 2 (score > 0,450) AND deleterious with Sift (score < 0.05), or (ii) probably damaging with Polyphen 2 (score > 0,850) or (iii) deleterious with Sift (score < 0,02); BKA = bilateral kidney agenesis. Only variants absent in GnomAD were considered.

Table S3A. *Greb1l* mutant mice generated by CRISPR/Cas9 using sgRNAs targeting exon 3 or exon 17.

Mouse line	sgRNA[a]	Indel	Sex of the Founder
Greb1l-a	Exon 3	c.64_68delATAG	Male
Greb1l-b	Exon 3	c.69_70delAGinsCAT	Male
Greb1l-c	Exon 17	c.2406_2411delATTGC c.2391_2407del17bp	Male
Greb1l-d	Exon 17	c.2404_2409delGGATT	Male
Greb1l-e	Exon 17	c.2405insT	Female
Greb1l-f	Exon 17	c.2404delGinsTC c.2404_2407delGGA	Female
Greb1l-g	Exon 17	c.2402_2405delACGG	Female

Table S3B. Offspring of F2 (exon 3 mutants) and F1 (exon 17 mutants)

Male	Female	Generation	Number of litters	Number of pups	Genotype pups
Greb1l-a	*Greb1l-a*	F2	7	33	15 *Greb1l* +/+ 18 *Greb1l* +/- (delATAG)
Greb1l-b	*Greb1l-b*	F2	2	12	4 *Greb1l* +/+ 8 *Greb1l* +/- (delAGinsCAT)
Greb1l-c	*Greb1l-e*	F1	1	8	2 *Greb1l* +/+ 2 *Greb1l* +/- (delATTGC) 2 *Greb1l* +/- (del17bp) 2 *Greb1l* +/- (insT)
Greb1l-c	*Greb1l-f*	F1	2	13	2 *Greb1l* +/+ 2 *Greb1l* +/- (delGGA) 3 *Greb1l* +/- (delATTGC) 1 *Greb1l* +/- (del17bp) 2 *Greb1l* +/- (delGinsTC) 3 *Greb1l* -/- (delATTGC/delGGA)[b]
Greb1l-d	*Greb1l-g*	F1	1	5	3 *Greb1l* +/+ 2 *Greb1l* +/- (delACGG)

(a) Sequence of sgRNA targeting exon 3: 3'-TAGAAGCCTCGCTCAGATGT-5'; Sequence of sgRNA targeting exon 17: 3'-AGAAGGATCTTGCACGACAG-5'. The sgRNAs were designed using the online tool "CRISPOR" (http://crispor.tefor.net).

(b) Compound heterozygous pups carrying an in-frame 3 bp deletion in addition to a 5 bp deletion.

Supplementary References

1. Adzhubei, I.A., Schmidt, S., Peshkin, L., Ramensky, V.E., Gerasimova, A., Bork, P., Kondrashov, A.S., and Sunyaev, S.R. (2010). A method and server for predicting damaging missense mutations. Nat. Methods *7*, 248-249.

2. Kumar, P., Henikoff, S., and Ng, P.C. (2009). Predicting the effects of coding nonsynonymous variants on protein function using the SIFT algorithm. Nat. Protoc. *4*, 1073-1081.

3. Grantham, R. (1974). Amino acid difference formula to help explain protein evolution. Science *185*, 862-864.

4. Kircher, M., Witten, D.M., Jain, P., O'Roak, B.J., Cooper, G.M., Shendure, J. (2014). A general framework for estimating the relative pathogenicity of human genetic variants. Nat. Genet. *46*, 310-315.

5. Houdayer, C. (2011). In silico prediction of splice-affecting nucleotide variants. Methods Mol. Biol. *760*, 269-281.